water

MDPI

Article

Hybrid Approach of Unmanned Aerial Vehicle and Unmanned Surface Vehicle for Assessment of Chlorophyll-a Imagery Using Spectral Indices in Stream, South Korea

Eun-Ju Kim, Sook-Hyun Nam, Jae-Wuk Koo and Tae-Mun Hwang *

Korea Institute of Civil Engineering and Building Technology—Environment Research Institute, Goyangdae-ro, Goyang-si 10223, Korea; kej@kict.re.kr (E.-J.K.); fpnsh@kict.re.kr (S.-H.N.); koojaewuk@kict.re.kr (J.-W.K.)
* Correspondence: taemun@kict.re.kr; Tel.: +82-31-910-0741

Abstract: The purpose of this study is to compare the spectral indices for a two-dimensional river algae map using an unmanned aerial vehicle (UAV) and an unmanned surface vehicle (USV) hybrid system. The UAV and USV hybrid systems can overcome the limitation of not being able to effectively compare images of the same region obtained at different times and under different seasonal conditions, when using a method of comparing and analyzing with absolute values in remote sensing. Radiometric correction was performed to minimize the interference that could distort the analysis results of the UAV imagery, and the images were taken under weather conditions that would minimally affect them. Three spectral indices, namely, normalized difference vegetation index (NDVI), normalized green–red difference index (NGRDI), green normalized difference vegetation index (GNDVI), and normalized difference red edge index (NDRE) were compared for the chlorophyll-a images. In field application and correlational analysis, the NDVI was strongly correlated with chlorophyll-a (R^2 = 0.88, $p < 0.001$), and the GNDVI was moderately correlated with chlorophyll-a (R^2 = 0.74, $p < 0.001$). As a result of comparing the chlorophyll-a concentration with the in-situ chlorophyll-a imagery by UAV, we obtained the RMSE of NDVI at 2.25, and the RMSE of GNDVI at 3.41.

Keywords: chlorophyll-a imagery; river; spectral indices; unmanned aerial vehicle; unmanned surface vehicle

Citation: Kim, E.-J.; Nam, S.-H.; Koo, J.-W.; Hwang, T.-M. Hybrid Approach of Unmanned Aerial Vehicle and Unmanned Surface Vehicle for Assessment of Chlorophyll-a Imagery Using Spectral Indices in Stream, South Korea. *Water* **2021**, *13*, 1930. https://doi.org/10.3390/w13141930

Academic Editor: Giuseppe Pezzinga

Received: 31 May 2021
Accepted: 5 July 2021
Published: 13 July 2021

1. Introduction

Algal blooms are natural phenomena that occur in water-based ecosystems in response to environmental factors, such as nutrition, light, water temperature, and wind speed [1]. Harmful algal blooms can cause substantial water quality problems that persist in rivers, lakes, and reservoirs [2–4]. Accordingly, monitoring the algae in rivers, lakes, and other freshwater bodies is proving to be an increasingly concerning issue. Of the various types of algae, blue–green algae are particularly concerning because of the potential existence of toxins within them, necessitating a fundamental solution for their reduction, to avoid economic and social problems [5,6]. Data pertaining to green algae hot-spots need to be collected quickly and frequently, because green algae exhibits repeated cycles of growth and death depending on environmental conditions such as light (solar radiation), water temperature, nutritional salts (nitrogen, phosphorus), and their duration of residence [1].

Chlorophyll-a is one of the photosynthetic pigments contained in algae, and it has traditionally been used as an indicator of algal biomass via field sampling to monitor algal growth. Fixed chlorophyll-a sensors are currently installed in South Korea to monitor sites, such as major water sources, rivers, and lakes, using an automatic water quality monitoring network [7]. Field sampling and assessment of algae is also conducted to monitor chlorophyll-a concentration levels and measure algal biomass [8]. However, monitoring via field sampling and chlorophyll-a concentration measurement can be problematic with

regards to temporal and spatial resolution, because the locations and/or compositions of large-scale algal outbreaks can change dramatically in a short time, due to multiple ubiquitous factors such as the rain and wind. In an effort to address this issue, recent studies have investigated the use of an unmanned aerial vehicle (UAV) to monitor chlorophyll-a concentration [9–14]. Because most images acquired by the UAV for analysis are taken from a distance of 50–200 m, atmospheric correction is not necessary, and multispectral sensors have proven to be effective for environmental monitoring [15–19].

A recent study has shown that using a UAV operating at an altitude of 50–300 m helped to remove interference, which distorts the remote sensing analysis results and evaluates the image quality of the images obtained under other weather conditions, and apply it in situ. In this case, the quality of the images obtained in cloudless and low-humidity areas was found to be good [20–22]. UAVs operating at low altitudes have greatly reduced the atmospheric correction requirements compared to satellites operating outside the atmosphere, or aerial vehicles operating at high altitudes [23].

The simplicity of operating a UAV makes it possible to adjust the capture time according to the solar angle position, based on the season, and the latitude and longitude of the capture point. It also makes it possible to change the operation schedule depending on whether there are cloudy or humid conditions. As a result of comparing the reflectivity and normalized distribution vegetation index (NDVI) of the UAV images obtained by flight path and time zone, in the case of reflectivity, there is a limit to the quantitative utilization, due to the large variability in the middle of day, on a daily basis without constant tendency, but the NDVI was reported to show a stable change of around 5%, without significant changes in the time series [24].

Several studies have been successful in quantifying concentration of chlorophyll-a or percent cover of aquatic vegetation with various algorithms [25–29]. The NDVI is one of many spectral indices [30] that has been used in this study [1,13,19].

To obtain chlorophyll-a images using an UAV, a chlorophyll-a concentration measurement must be performed in the target aquatic area, in conjunction with the UAV in situ. Data collection is required at various water points in situ. Traditionally, a boat has been required to measure the chlorophyll-a concentration in fairly inaccessible streams, but it is time and labor intensive, and entails numerous associated limitations. Therefore, it is necessary to develop a mobile, less cumbersome technology for an immediate water quality measurement in situ [31]. When remote sensing is performed, using a UAV equipped with a multispectral or hyperspectral sensor, accurate and repeatable results, especially in the entire procedure of processing the image obtained in different seasons and different lighting conditions, may not always be drawn. In particular, some studies do not take into account the time resolution, and there is a limit to the lack of accuracy of the image at the time of measurement when extracting the value of a specific wavelength band and interpreting the model as an absolute value [32].

To solve this problem, the analysis is required at the same time in the field, in order to be analyzed with relative values, and for this purpose, the study was used to develop unmanned surface vehicles (USV) to measure the in situ chlorophyll-a concentration. The USVs have garnered increasing interest in recent research and development. They are being used in a variety of research areas, including water quality monitoring, surveillance, underwater terrain mapping, and oceanography [33–42]. They also have applications in ameliorating space and time constraints, by automating data collection. Autonomous USV technology can be conducive to improving water quality monitoring methods [43].

In this study, the UAV spectral images were combined with in situ data that were obtained from the USV, to create chlorophyll-a images using UAV and USV hybrid platforms in the Nae Seong Stream in Korea. As well as the NDVI, the use of other spectral indices to estimate chlorophyll-a concentration were investigated. To date, few studies have investigated the development and application of USVs in conjunction with UAVs in the field of visual two-dimensional spatial distribution imagery of chlorophyll-a concentration. For this, relative values are derived by applying the spectral indices calculation formula for

the acquired images by band, after acquiring data from the stream in optimal conditions, using the UAV equipped with multispectral sensor. The values are corrected with in situ water quality measurements, obtained by the simultaneous operation of UAV and USV, and then image processed. This enhances not only the stability compared to estimating a model using the absolute value in remote sensing, but also the reliability of the analysis results, such as the time series changes by performing cross-validation and applying the experimental chlorophyll-a concentration measured in situ.

2. Materials and Methods

2.1. Study Area

The study site was located in the Nae Seong Stream (N Stream) in Korea (36°48′21″ N, 128°41′45″ E) (Figure 1). The N stream is of interest because algal blooms occur there every year. The UAV flight was targeted at 3.2 km, and the USV operated at 2.31 × 0.10 km^2. UAV flight and USV service took place almost at the same time.

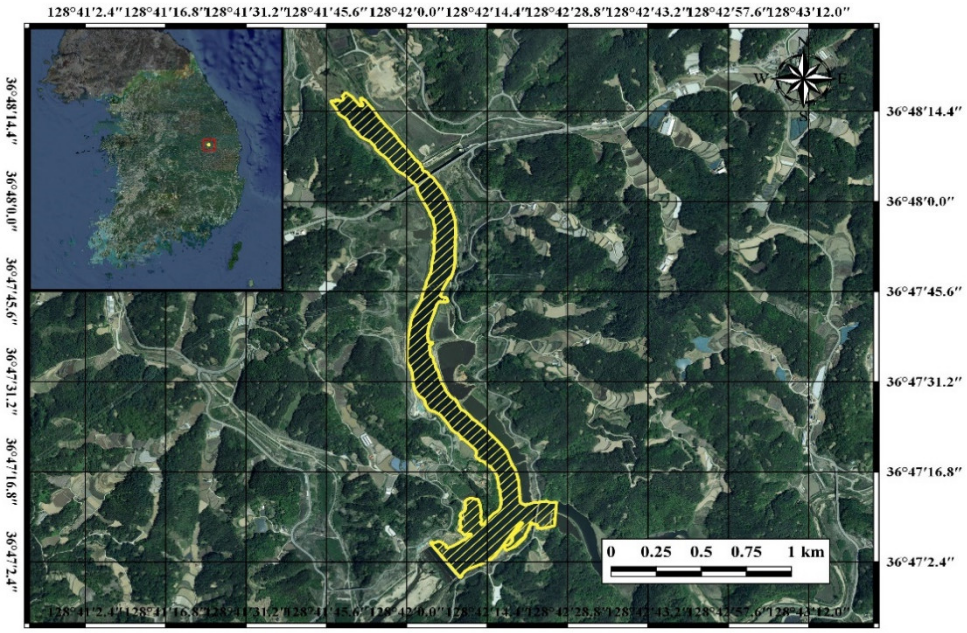

Figure 1. The study area (N Stream).

2.2. UAV Data Acquisition and Image Processing

The UAV (Remo-M by Uconsystem Inc., Daejon, Korea) used in the study is shown in Figure 2a. It has a wingspan of 1.8 m, and weighs 3.4 kg. It is equipped with a brushless AXI 2826/10 motor (Model Motors LTD., Hradec Králové, Czechia) and an Aeronaut carbon propeller (Aero-Naut^8, Reutlingen, Germany). Its maximum speed is 80 km/h and it has a minimum operating distance of 8 km. A Sequoia multispectral sensor (Parrot Cor., Paris, France) is mounted on the UAV. Four cameras in the sensor create multispectral images in the following four spectral bands: green (530–570 nm), red (640–680 nm), red edge (730–740 nm), and near-infrared (NIR) (770–810 nm). The focal length of the camera is 3.98 mm, image size is 1280 × 960 pixels, and sensor size is 4.8 × 3.6 mm. The UAV flight preparation begun on 18 September 2019 at 8:00 a.m. and was finished at 9:00 a.m. The images were taken under sunny conditions and clear skies, humidity ranged from 40 to 70%, and flight wind speed was 0–3 m/s to minimize any negative effects on images [22,44].

(**a**) (**b**)

Figure 2. The unmanned aerial vehicle and sensor used in the study: (**a**) the Remo-M and (**b**) the Sequoia multispectral sensor.

The altitude of the UAV takeoff point was 150 m. Data were collected from a 3.2 km section during a single 15-min flight. To ensure lateral overlap of ≥65% and longitudinal overlap of ≥75% the images were taken in four strips at an altitude of 150 m. The entire 15-min flight covering the 3.2 km section was photographed, with the camera set at 60-m strip intervals and a shooting interval of 2 s. For image identification, 15 ground control points (V100 GNSS, Hi Target, Shanghai, China) were installed around the site before the flight so that positional image displacement could be corrected.

In order to measure algae bloom using remote sensing, reflectance of water, which is a function of light scattering and absorption properties of water [16,45], is to be considered [46,47]. According to the results of the previous study about water reflectance, it was reported that water spectral changes regarding increasing the altitude up to 20–100 m using UAVs, without the confounding influence of atmospheric effects, could be ignored [48]. The previous study also reported that image radiometric quality is affected by meteorological conditions [20].

Recently, a study on accurately evaluating the radiometric quality of UAV imagery is underway, which will reduce the analytical potential of images and eliminate interference, which can distort the results of remote sensing analysis [19,47]. Since reflective data of the research area can be obtained directly after using sequoia image and processing it, it was reported that errors of spectral indices are correlated with a way of calibrating a level of radiation in the case that spectral indices are calculated using the reflective data of spectral indices equation [49].

In this study, radiometric calibration was performed using the Sequoia sensor module of Parrot Sequoia® (Parrot Drone SAS, Paris, France) and calibration target panel that include the pre-calibration process in multispectral cameras, as shown in Figure 3 [50].

(**a**) (**b**) (**c**)

Figure 3. Sequoia sensor module and calibration target panel: (**a**) Parrot Sequoia multispectral sensor, (**b**) multispectral sunshine sensor module, and (**c**) calibration target.

Parrot Sequoia® used in this study is a multispectral sunlight sensor that can record illumination information of each image, which makes it simple to calibrate a multispectral image. For this, calibration of a level of radiation using calibration panels provided by a manufacturing company is possible and reflective data can be directly obtained. The formula for radiation calibration is available from the Parrot Sequoia [51]. This is termed as reflectance target/tarp/panel calibration. Radiometric correction was performed in the option 'Radiometric processing and calibration' of Pix4D. The photographs were pro-

cessed using orthomosaics, georeferenced digital surface models, and the two-dimensional mapping software Pix4D (Lausanne, Switzerland). At the initial processing stage, external distortions caused by the UAV tilting and internal distortions caused by camera characteristics were corrected, and photo junction points were extracted via a scale-invariant key point algorithm [51].

2.3. USV Data Acquisition and Processing

The USV used in the study was developed by our research team specifically for monitoring chlorophyll-a concentration in the N Stream, and it is shown in Figure 4a. It is 1.3 m long, weighs approximately 10 kg, and can operate at a maximum speed of 18 km/h. The communication distance is 2–3 km or more, at a frequency of 2.400–2.483 GHz. In addition to a general camera sensor, it also included an echo sound apparatus for measuring the depth of the river, a light detection and ranging (Lidar) sensor to prevent collisions, and the AlgaeChek Ultra (Modern Water, London, UK) fluorometer for the measurement of chlorophyll-a concentration.

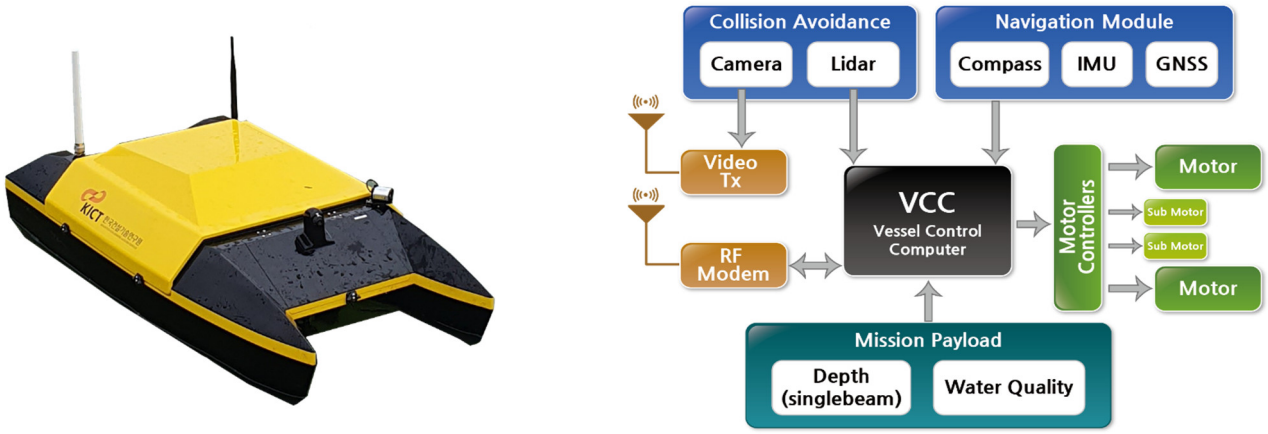

(**a**) (**b**)

Figure 4. The unmanned surface vehicle used in the study: (**a**) unmanned surface vehicle and (**b**) architecture.

Portable fluorometers that can measure chlorophyll-a concentration in situ include AlgaeChek Ultra (Modern Water, London, UK), nanoFlu (TriOS, Rastede, German), and TriLux (Chelsea, Surrey, UK). The features of the portable fluorometer are that it is low cost and the wireless data transmission by means of RS-232 is convenient. In this study, AlgaeChek Ultra was applied, chlorophyll-a concentration measurement range was set as 0–100 μg/ L, and other turbidity and phycocyanin factors were measured. In this study, the sensor was used only after prior testing. Chlorophyll-a concentrations were recorded in the sensor in μg/L.

Chlorophyll-a sensor mounted on USV was tested before operation. Rhodamine B (Sigma-Aldrich, Saint Louis Zoo, USA) 0.25, 0.5, 1, 2 μM was manufactured and measured, and is used to confirm whether a signal is properly transmitted.

The water quality sensor is mounted at a location on the vehicle that is not affected by the propeller. The location receiving system consists of the global navigation satellite system L1 (GNSS) and a satellite-based augmentation system-class receiver of 5 Hz or higher. An autonomous navigation program is used to set the unmanned travel route. The main operation modes and functions are autonomous route operation, point navigation, and automatic return. The maximum operation time is approximately 5 h. The water quality sensor and location data are synchronized with the flight control computer via a parsing protocol, and are stored in real time.

The architecture of the USV system is shown in Figure 4b. The USV continuously measured chlorophyll-a concentration during autonomous operation within a 2.31 × 0.10 km^2

area along in the N Stream. The route width was 20 m and the operating speed of the USV was 1.6 km/h.

In situ chlorophyll-a concentration data were obtained from the N Stream by the USV as it traveled the route shown in Figure 5. Because raw data obtained from the USV are extensive, they must be processed prior to being compared with the UAV-derived image data. USV data obtained from in situ can perform exploratory data analysis (EDA). EDA is a technique that performs analysis using a variety of visualization methods, such as histograms, acidity, and correlation analysis, to determine how the data are distributed with a large amount of data processing technology, and whether there is correlation of the data [52]. For the extraction of extensive raw data, this study was used to develop a data analysis tool (DAT). This software written in the C# and R. In this study, it was customized to compile code and run on Windows. DAT can extract chlorophyll-a concentration data at desired coordinates and distance intervals, with the exception of outlier data. Analytical data from USV are used to obtain spectral indices of images taken during UAV flight and relative expressions of chlorophyll-a concentration.

Figure 5. The operator's remote interface for operating route in the N Stream.

2.4. Chlorophyll-a Spectral Indices

The previously described multispectral indices that have been used as indicators of algal blooms in rivers [30], shown in Table 1, were used to generate UAV images of chlorophyll-a concentration. The chlorophyll-a concentrations were measured by the APHA 10200-H method [53].

Table 1. Spectral indices used for chlorophyll-a assessment in the current study.

Name	Derivation	References
Normalized difference vegetation index (NDVI)	(NIR * − red)/(NIR + red)	[54]
Normalized green–red difference index (NGRDI)	(green − red)/(green + red)	[55]
Green normalized difference vegetation index (GNDVI)	(NIR − green)/(NIR + green)	[56,57]
Normalized difference red edge index (NDRE)	(NIR − red edge)/(NIR + red edge)	[58]

* NIR, near-infrared.

The indices applied in the present study were the NDVI, the normalized green–red difference index (NGRDI), the green normalized difference vegetation index (GNDVI), and the normalized difference red edge index (NDRE).

2.5. Methodology Flowchart

A flowchart representing the UAV imaging and image analysis procedures used in the study is shown in Figure 6. The two main components were imaging performed by the UAV (sky zone), and in situ water quality analysis performed by the USV (surface zone). Spectral indices were extracted from the image analysis data acquired via flight photogrammetry, chlorophyll-a concentration estimations derived from USV data were collated, and the combination of the two was used to generate a regression equation. Coefficient of determination (R^2) was then estimated to determine whether to create chlorophyll-a concentration imagery.

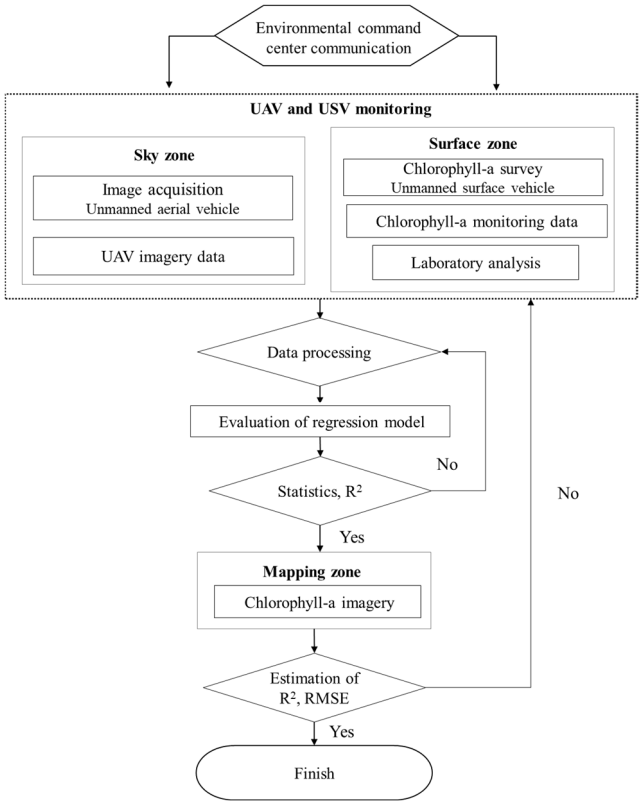

Figure 6. Methodological flowchart using UAV and USV hybrid system.

The suitability of the linear regression analysis of the correlation between the spectral indices obtained using the UAV and the in-situ chlorophyll-a data obtained using the USV was evaluated, with the R^2 at a significance level of $p < 0.001$.

The most common way to compare completed chlorophyll-a imagery is to compare it through statistical regression of the actual in situ concentration, by means of chlorophyll-a and USV of the completed imagery. The completed imagery is compared with the USV in situ data (surface zone). Suitability is defined by the coefficient R^2 and root mean square error (RMSE). RMSE equation is the same as (1).

$$RMSE = \sqrt{\frac{\sum_i^n (y - yi)^2}{n}} \quad (1)$$

Here, y is USV data, yi is chlorophyll-a image completed by spectral indices. If R^2 and RMSE are not satisfactory, data analysis must be performed again from the beginning.

3. Results

3.1. USV Data Analysis

As seen in the histogram in Figure 7a, the chlorophyll-a data obtained by the USVs have a right-skewed distribution. The box plot (Figure 7b) shows a maximum value of data, first quartile, third quartile, median, minimum, maximum, and distribution of data. Outliers exist; however, it is possible to identify values that are too large or small compared to the other values of the observed value. The normal distribution and interquartile range were considered for outlier removal. As a result, out-of-place was used as a quartile (first quartile, 75% third quartile) method. The lower quartile was defined as zero and data that were out of the permissible range, the upper quartile, 48.7 μg/L, was defined as the outliers. The number of data contained by operating the USV was 242,818, and the number of outlier removals was 228,259. The range of chlorophyll-a concentration of raw data was −3.5–100.9 μg/L, and the range of chlorophyll-a concentration after removing the outlier was 1.0–48.7 μg/L.

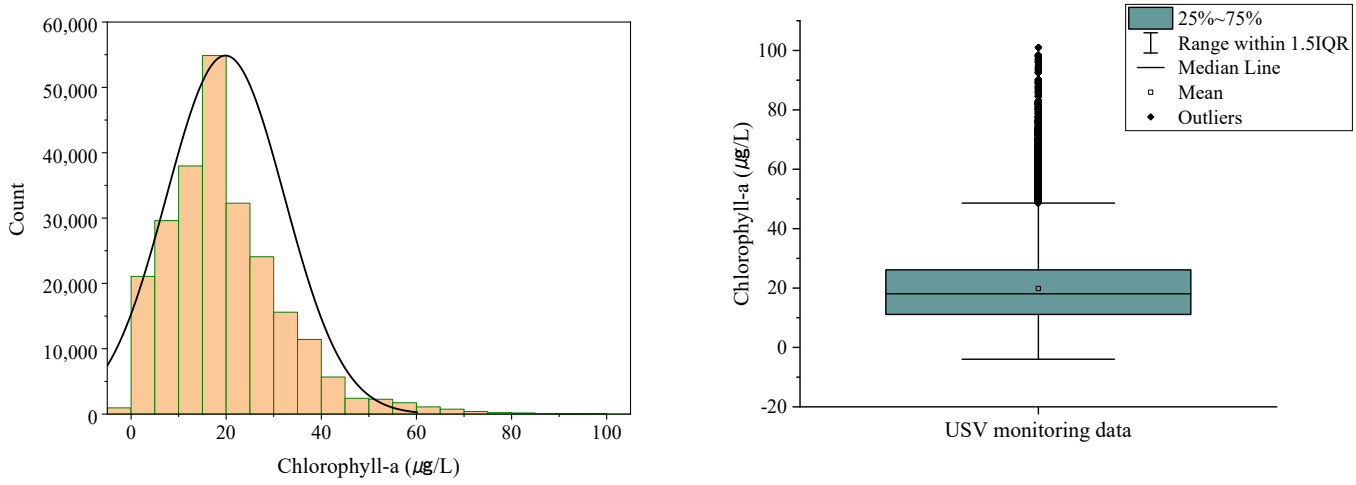

Figure 7. Histogram and box plot of chlorophyll-a in monitoring site: (**a**) histogram, and (**b**) box plot.

In Figure 8, the concentration of chlorophyll-a measured by USV was compared with the data directly collected from the field. The chlorophyll-a concentration, measured with laboratory analysis and in situ sensors, was found to have $R^2 = 0.92$, $p < 0.005$. As a result of the analysis, it was shown that the chlorophyll-a concentration measured with laboratory analysis was higher than that measured by the sensor in situ.

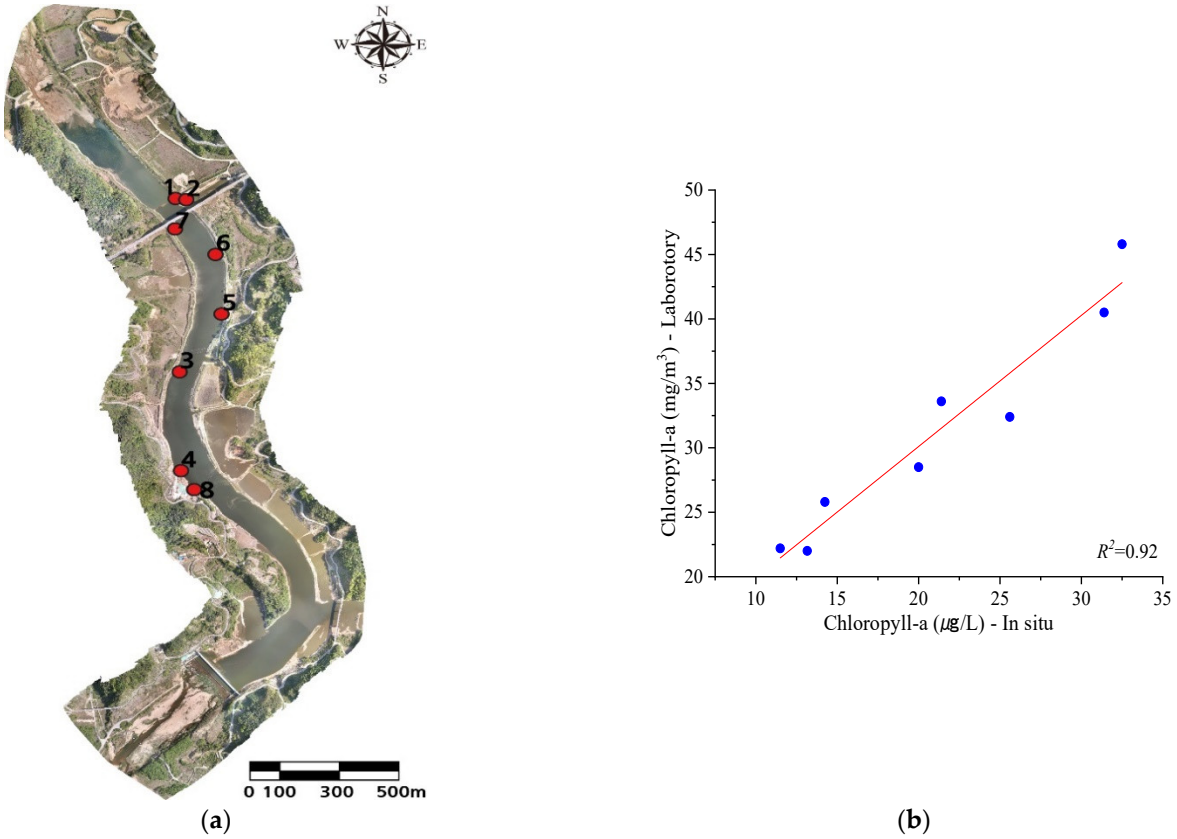

(**a**) (**b**)

Figure 8. Laboratory data versus sensor data for chlorophyll-a concentration: (**a**) sampling points, (**b**) correlation.

3.2. Spectral Indices Analysis

In this study, after filming in optimal conditions using a UAV equipped with multi-spectral sensors, spectral indices were extracted per band from the obtained images. The Chlorophyll-a concentration was extracted by correlation model of spectral index data obtained through UAV and water quality data from USV. This improves the reliability of the analysis results, by performing cross-validation and applying an experimental value, while the USV and UAV are operated simultaneously. The stability is also compared to the remote sensing method, to derive a value using the absolute value. The chlorophyll-a concentration data, measured by the USV using the developed DAT, are used for the correlation analysis of the spectral indices of the image taken during the UAV flight. The chlorophyll-a data acquired by the USV sensor were extracted at intervals of 80 m.

In this study, we observed the four different indices (band ration algorithms), which were used to identify the chlorophyll-a concentrations as indicators of algae bloom from the UAV images. The results of the correlational analysis between the four spectral indices and the in situ chlorophyll-a concentration measurements, obtained via the USV, are shown in Figure 9. These indices include NDVI, GNDVI, NGRDI, and NDRE. The NDVI and GNDVI showed lower values than the NGRDI and NDRE. The chlorophyll-a concentration was greatly correlated with the NDVI (R^2 = 0.88, $p < 0.001$) and GNDVI (R^2 = 0.74, $p < 0.001$). It was not correlated with the NGRDI (R^2 = 0.004) or NDRE (R^2 = 0.04). As shown in Figure 9, the GNDVI and NDVI have high correlations, while the NGRDI and NDRE show the lowest correlations. These results demonstrate that although the NDVI reflects the characteristics of chlorophyll-a better than the GNDVI in the remote detection, the GNDVI can be also used to estimate the chlorophyll-a concentration. In other words, chlorophyll-a can be estimated by identifying the green band, in addition to the red and NIR bands. The imagery of chlorophyll-a, derived using the NDVI and the GNDVI, are shown in Figure 10.

The analyses using these indices indicated that the level of chlorophyll-a concentration in the N Stream was in the range of 0–45 μg/L.

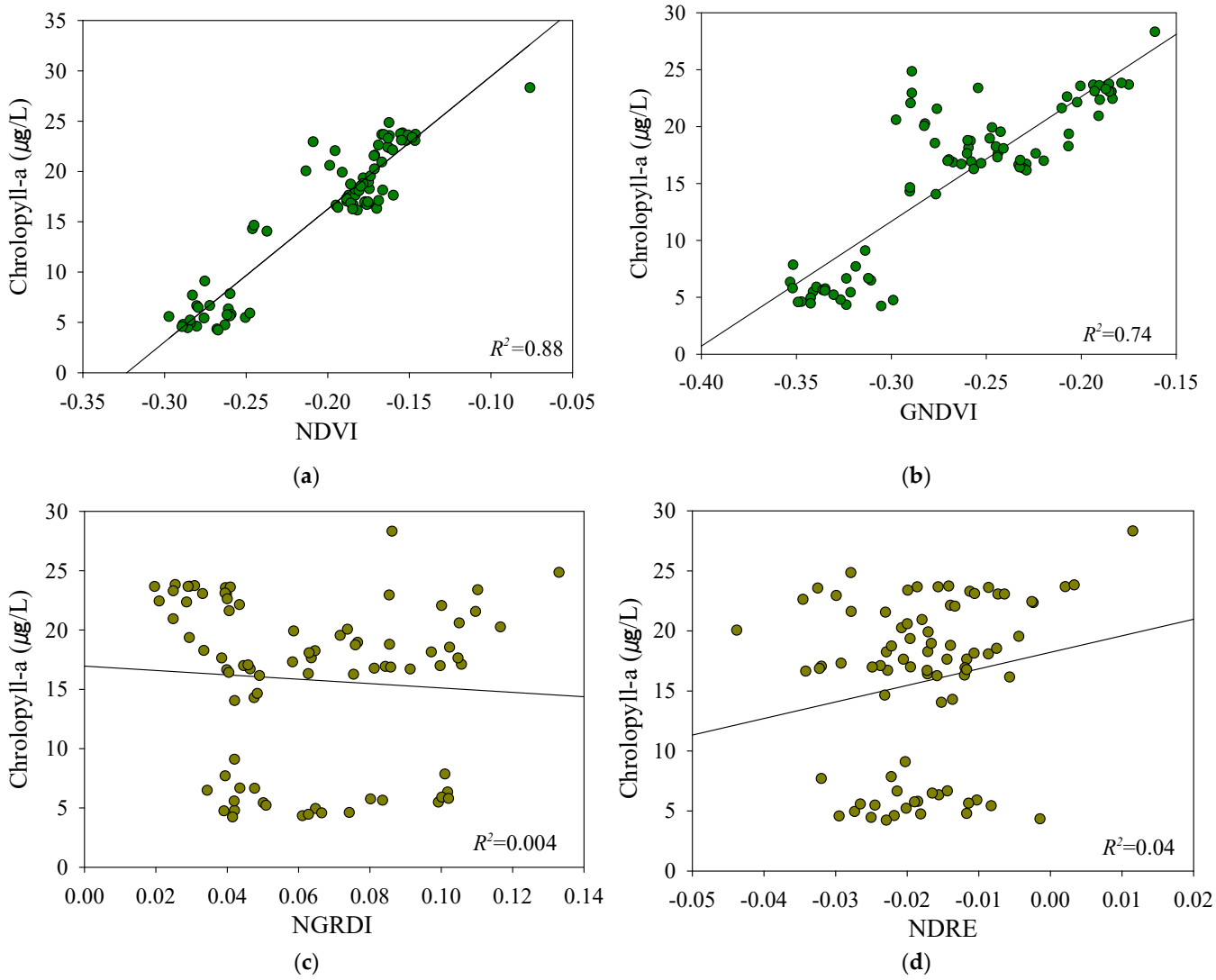

Figure 9. Regression analysis of the four spectral indices and chlorophyll-a: (**a**) normalized difference vegetation index (NDVI), (**b**) green normalized difference vegetation index (GNDVI), (**c**) normalized green–red difference index (NGRDI), and (**d**) normalized difference red edge index (NDRE).

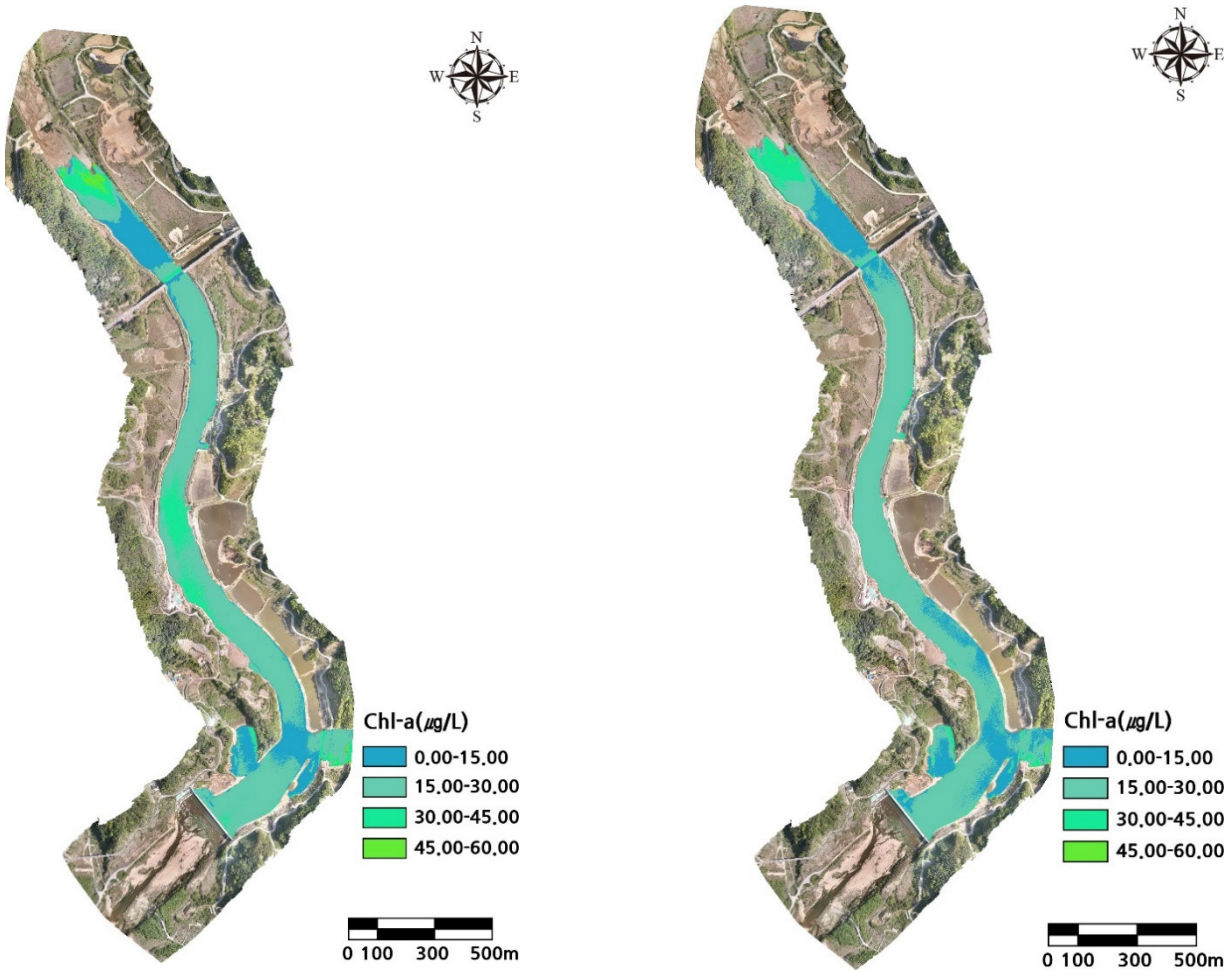

Figure 10. Chlorophyll-a (chl-a) imagery derived using (**a**) the normalized difference vegetation index (NDVI), and (**b**) the green normalized difference vegetation index (GNDVI).

Figure 11 showed the correlation between chlorophyll-a concentration extracted from the NDVI or GNDVI and measured data by USV. As a result of being compared with the actual data of the NDVI, R^2 = 0.88 and RMSE = 2.25. As a result of being compared with the actual data of the GNDVI, R^2 = 0.73 and RMSE = 3.41. The NDVI and GNDVI, which showed the most apparent difference between aquatic vegetation and water surface, were reported to be the most effective for detecting aquatic plants [54].

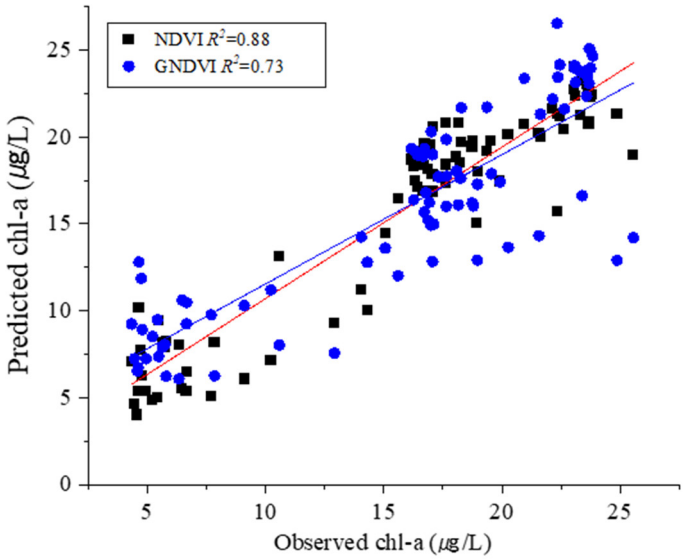

Figure 11. Comparison of chlorophyll-a concentration calculated by NDVI and GNDVI.

4. Discussion

The UAV and USV hybrid platforms, which use multispectral sensors and water quality sensors to detect, and chlorophyll-a concentration imagery as an indicator for algal blooms, provide more reliable spatial information than either one alone and help identify specific algal species. The NDVI and GNDVI were also reported to be effective indices in a previous study, which was conducted on the detection of chlorophyll-a concentration using vegetation indices and images obtained from a multispectral sensor-integrated UAV [33]. The NDVI and GNDVI can be used to estimate chlorophyll-a because of the identification of the green band; however, the red and NIR bands also facilitate the estimation of chlorophyll-a. These results were similar to previous studies, in which vegetation indices were applied to detect the chlorophyll-a concentration in water. Collecting and analyzing large amounts of in situ data, in order to image chlorophyll-a concentration using vegetation indices with more reliable spectral resolution, is critical [55]. Furthermore, when imaging chlorophyll-a concentration in water, the analysis results may be distorted by wave distortion, solar reflection, shadow, turbidity, etc. Regardless of which sensor is used, a large amount of chlorophyll-a concentration data must be obtained on the ground, continuously, during the same flight period. Because chlorophyll-a shows different reflected signals depending on its seasonal or visual appearance, the chlorophyll-a concentration was measured at numerous points of the target water body, using the USV during the flight time of the UAV. When remote sensing is performed, the method in which the UAV and USV are used simultaneously can be an advantageous, because relative values are compared rather than absolute values. In the results of analyzing the chlorophyll-a concentration that was measured using the USV, and various vegetation indices extracted from the multispectral images of the UAV, the NDVI showed a very high correlation in terms of representing the characteristics of chlorophyll-a concentration in the water.

5. Conclusions

To show chlorophyll-a imagery with relative values using UAVs, in situ analysis must be performed in the target waters, along with UAV measurements. When remote sensing is performed, the method of utilizing the UAV and USV simultaneously proves to be an advantage of using in situ data, in which case the comparison analysis is done with relative values rather than absolute values.

In this study, a UAV and an autonomous USV hybrid system were developed, in order to assess the chlorophyll-a concentration imagery. The use of autonomous USVs has enabled successful acquisition of a reliable chlorophyll-a concentration in situ. The DAT

was adapted and used in the analysis of the USV data, and three types of spectral indices were applied to the UAV images to derive estimations of the chlorophyll-a concentration. The chlorophyll-a imagery, thus derived, indicated that both the NDVI and GNDVI were useful.

In this study, the UAV and USV hybrid system has been successfully applied for high-resolution two-dimensional images so far, and, in the future, an attempt will be made to create a three-dimensional image combined with a river water quality model.

Author Contributions: Conceptualization, E.-J.K.; methodology, S.-H.N.; software, E.-J.K.; investigation, J.-W.K. and T.-M.H.; data curation, S.-H.N.; writing—original draft preparation, E.-J.K.; writing—review and editing, S.-H.N. and E.-J.K.; supervision, T.-M.H.; funding acquisition, T.-M.H. All authors have read and agreed to the published version of the manuscript.

Funding: This study was funded by the major project of the Korea Institute of Civil Engineering and Building Technology (KICT) (grant number 20210106-001).

Data Availability Statement: Not applicable.

Acknowledgments: We would like to thank M.S. Lee for their support, as well as H.S. Han for invaluable suggestions to the manuscript.

Conflicts of Interest: The authors declare no conflict of interest.

References

1. Van der Merwe, D.; Price, K.P. Harmful algal bloom characterization at ultra-high spatial and temporal resolution using small unmanned aircraft systems. *Toxins* **2015**, *27*, 1065–1078. [CrossRef]
2. Hallegraeff, G.M.A. Review of harmful algal blooms and their apparent global increase. *Phycologia* **1993**, *32*, 79–99. [CrossRef]
3. Preece, E.P.; Hardy, F.J.; Moore, B.C.; Bryan, M.A. Review of microcystin detections in Estuarine and Marine waters: Environmental implications and human health risk. *Harmful Algae* **2017**, *61*, 31–45. [CrossRef]
4. Shen, Q.; Zhu, J.; Cheng, L.; Zhang, Z.; Xu, Z. Enhanced algae removal by drinking water treatment of chlorination coupled with coagulation. *Desalination* **2011**, *271*, 236–240. [CrossRef]
5. Teixeira, M.R.; Rosa, M.J. Comparing dissolved air flotation and conventional sedimentation to remove cyanobacterial cells of Microcystis aeruginosa: Part I: The key operating conditions. *Sep. Purif. Technol.* **2006**, *52*, 84–94. [CrossRef]
6. Figueiredo, D.R.; Azeiteiro, U.M.; Esteves, S.M.; Gon Alves, F.J.M.; Pereira, M.J. Microcystin-producing blooms—A serious global public health issue 1. *Ecotoxicol. Environ. Saf.* **2004**, *59*, 151–163. [CrossRef]
7. Jung, K.Y.; Lee, K.L.; Im, T.H.; Kee, I.J.; Kim, S.; Han, K.T.; Ahn, J.M. Evaluation of water quality for the Nakdong River watershed using multivariate analysis. *Environ. Technol. Innov.* **2016**, *5*, 67–82. [CrossRef]
8. Gregor, J.; Marlek, B. Freshwater phytoplankton quantification by chlorophyll-a: A comparative study of in vitro, in vivo and in situ methods. *Water Res.* **2004**, *38*, 517–522. [CrossRef] [PubMed]
9. Watanabea, Y.; Kawaharab, Y. UAV photogrammetry for monitoring changes in river topography and vegetation. *Procedia Eng.* **2016**, *154*, 317–325. [CrossRef]
10. Flynn, K.F.; Chapra, S.C. Remote sensing of submerged aquatic vegetation in a shallow non-turbid river using an unmanned aerial vehicle. *Remote Sens.* **2014**, *6*, 12815–12836. [CrossRef]
11. Pajares, G. Overview and current status of remote sensing applications based on unmanned aerial vehicles (UAVs). *Photogramm. Eng. Remote Sens.* **2015**, *81*, 281–329. [CrossRef]
12. Su, T.C.; Chou, H.T. Application of multispectral sensors carried on unmanned aerial vehicle (UAV) to trophic state mapping of small reservoirs: A case study of Tain-Pu reservoir in Kinmen. *Taiwan. Remote Sens.* **2015**, *7*, 10078–10097. [CrossRef]
13. Zaman, B.; Jensen, A.; Clemens, S.R.; McKee, M. Retrieval of spectral reflectance of high resolution multispectral imagery acquired with an autonomous unmanned aerial vehicle. *Photogramm. Eng. Remote Sens.* **2014**, *80*, 1139–1150.
14. Becker, R.H.; Sayers, M.; Dehm, D.; Shuchman, R.; Quintero, K.; Bosse, K.; Sawtell, R. Unmanned aerial system based spectroradiometer for monitoring harmful algal blooms: A new paradigm in water quality monitoring. *J. Great Lakes Res.* **2019**, *45*, 444–453. [CrossRef]
15. Zarco-Tejada, P.J.; González-Dugo, V.; Berni, J.A.J. Fluorescence, temperature and narrow-band indices acquired from a UAV platform for water stress detection using a micro-hyperspectral imager and a thermal camera. *Remote Sens. Environ.* **2012**, *117*, 322–337. [CrossRef]
16. Richardson, L.L. Remote sensing of algal bloom dynamics. *BioScience* **1996**, *46*, 492–501. [CrossRef]
17. Aguirre-Gómez, R.; Salmerón-García, O.; Gómez-Rodríguez, G.; Peralta-Higuera, A. Use of unmanned aerial vehicles and remote sensors in urban lakes studies in Mexico. *Int. J. Remote. Sens.* **2017**, *38*, 2771–2779. [CrossRef]
18. Tong, A.; He, Y. Estimating and mapping chlorophyll content for a heterogeneous grassland: Comparing prediction power of a suite of vegetation indices across scales between years. *ISPRS J. Photogramm. Remote Sens.* **2017**, *126*, 146–167. [CrossRef]

19. Mishra, S.; Mishra, D.R. Normalized difference chlorophyll index: A novel model for remote estimation of chlorophyll-a concentration in turbid productive waters. *Remote Sens. Environ.* **2012**, *117*, 394–406. [CrossRef]
20. Kedzierski, M.; Wierzbicki, D.; Sekrecka, A.; Fryskowska, A.; Walczykowski, P.; Siewert, J. Influence of lower atmosphere on the radiometric quality of unmanned aerial vehicle imagery. *Remote Sens.* **2019**, *11*, 1214. [CrossRef]
21. Deng, L.; Tan, Y.; Gong, H.; Duan, F.; Zhong, R. The effect of spatial resolution on radiometric and geometric performances of a UAV-mounted hyperspectral 2D imager. *ISPRS J. Photogramm. Remote Sens.* **2018**, *144*, 298–314. [CrossRef]
22. Brede, B.; Suomalainen, J.; Bartholomeus, H.; Herold, M. Influence of solar zenith angle on the enhanced vegetation index of a Guyanese rainforest. *Remote Sens. Lett.* **2015**, *6*, 972–981. [CrossRef]
23. Zeng, C.; Richardson, M.; King, D.J. The impacts of environmental variables on water reflectance measured using a lightweight unmanned aerial vehicle (UAV)-based spectrometer system. *J. Photogramm. Remote Sens.* **2017**, *130*, 217–230. [CrossRef]
24. Fawcett, D.; Panigada, C.; Tagliabue, G.; Boschetti, M.; Celesti, M.; Evdokimov, A.; Biriukova, K.; Colombo, R.; Miglietta, F.; Rascher, U.; et al. Multi-scale evaluation of drone-based multispectral surface reflectance and vegetation indices in operational conditions. *Remote Sens.* **2020**, *12*, 514. [CrossRef]
25. Choe, E.Y.; Lee, J.W.; Lee, J.K. Estimation of chlorophyll-a concentrations in the Nakdong River using high-resolution satellite image. *Korean J. Remote Sens.* **2011**, *27*, 613–623. [CrossRef]
26. Chen, L.; Tan, C.H.; Kao, S.J.; Wang, T.S. Improvement of remote monitoring on water quality in a subtropical reservoir by incorporating grammatical evolution with parallel genetic algorithms into satellite imagery. *Water Res.* **2008**, *42*, 296–306. [CrossRef]
27. Gitelson, A.A.; Dall'Olmo, G.; Moses, W.; Rundquist, D.C.; Barrow, T.; Fisher, T.R.; Gurlin, D.; Holz, J. A simple semi-analytical model for remote estimation of chlorophyll-a in turbid waters: Validation. *Remote Sens. Environ.* **2008**, *112*, 3582–3593. [CrossRef]
28. Brezonik, P.; Menken, K.D.; Bauer, M. Landsat-based remote sensing of lake water quality characteristics, including chlorophyll and colored dissolved organic matter (CDOM). *Lake Reserv. Manag.* **2005**, *21*, 373–382. [CrossRef]
29. Tebbs, E.J.; Remedios, J.J.; Harper, D.M. Remote sensing of chlorophyll-a as a measure of cyanobacterial biomass in Lake Bogoria, a hypertrophic, saline-alkaline, flamingo lake, using Landsat ETM+. *Remote Sens. Environ.* **2013**, *135*, 92–106. [CrossRef]
30. Kislik, C.; Dronova, I.; Kelly, M. UAVs in support of algal bloom research: A review of current applications and future opportunities. *Drones* **2018**, *2*, 35. [CrossRef]
31. Ferri, G.; Manzi, A.; Fornai, F.; Ciuchi, F.; Laschi, C. The HydroNet ASV, a small-sized autonomous catamaran for real-time monitoring of water quality: From design to missions at sea. *IEEE J. Ocean. Eng.* **2015**, *40*, 710–726. [CrossRef]
32. Tu, Y.H.; Phinn, S.; Johansen, K.; Robson, A. Assessing radiometric correction approaches for multi-spectral UAS imagery for horticultural applications. *Remote Sens.* **2018**, *10*, 1684. [CrossRef]
33. Naeem, W.; Sutton, R.; Chudley, J. Soft computing design of a linear quadratic Gaussian controller for an unmanned surface vehicle. In Proceedings of the 14th Mediterranean Conference on Control and Automation, Ancona, Italy, 28–30 June 2006; pp. 1–6.
34. Demetillo, A.T.; Taboada, E.B. Real-time water quality monitoring for small aquatic area using unmanned surface vehicle. *ETASR* **2019**, *9*, 3959–3964. [CrossRef]
35. Arzamendia, M.; Espartza, I.; Reina, D.G.; Toral, S.L.; Gregor, D. Comparison of Eulerian and Hamiltonian circuits for evolutionary-based path planning of an autonomous surface vehicle for monitoring Ypacarai Lake. *JAIHC* **2019**, *10*, 1495–1507. [CrossRef]
36. Manley, J.E. Unmanned maritime vehicles, 20 years of commercial and technical evolution. In *Oceans 2016 MTS/IEEE Monterey*; IEEE: New York, NY, USA, 2016; Volume 9, pp. 19–23.
37. Bayat, B.; Crasta, N.; Crespi, A.; Pascoal, A.M.; Ijspeert, A. Environmental monitoring using autonomous vehicles: A survey of recent searching techniques. *Curr. Opin. Biotechnol.* **2017**, *45*, 76–84. [CrossRef] [PubMed]
38. Wiora, J.; Kozyra, A.; Wiora, A. Towards automation of measurement processes of surface water parameters by a remote-controlled catamaran. *Bull. Pol. Acad. Sci. Tech. Sci.* **2017**, *65*, 351–359. [CrossRef]
39. Fornai, F.; Ferri, G.; Manzi, A.; Ciuchi, F.; Bartaloni, F.; Laschi, C. An autonomous water monitoring and sampling system for small-sized ASVs. *IEEE J. Ocean. Eng.* **2017**, *42*, 5–12.
40. Mousazadeh, H.; Hamid, J.; Elham, O.; Farshid, M.; Ali, K.; Yousef, S.; Ashkan, M. Experimental evaluation of a hydrography surface vehicle in four navigation modes. *J. Ocean Eng. Technol.* **2017**, *2*, 127–136. [CrossRef]
41. Rabah, F.K.J.; Ghabayen, S.M.; Salha, A.A. Effect of GIS interpolation techniques on the accuracy of the spatial representation of groundwater monitoring data in Gaza Strip. *J. Environ. Sci. Technol.* **2011**, *4*, 579–589. [CrossRef]
42. Goldberg, S.J.; Kirby, J.T.; Licht, S.C. *Applications of Aerial Multi-Spectral Imagery for Algal Bloom Monitoring in Rhode Island*; SURFO Technical Report No. 16-01; University of Rhode Island: South Kingstown, RI, USA, 2016; Volume 28.
43. Mantzafleri, N.; Psilovikos, A.; Blanta, A. Water quality monitoring and modeling in Lake Kastoria, using GIS. Assessment and management of pollution sources. *Water Resour. Manag.* **2009**, *23*, 3221–3254. [CrossRef]
44. Pan, Z.; Zhang, H.; Min, X.; Xu, Z. Vicarious calibration correction of large FOV sensor using BRDF model based on UAV angular spectrum measurements. *J. Appl. Remote Sens.* **2020**, *14*, 027501. [CrossRef]
45. Brown, C.A.; Huot, Y.; Werdell, P.J.; Gentili, B.; Claustre, H. The origin and global distribution of second order variability in satellite ocean color. *Remote Sens. Environ.* **2008**, *112*, 4186–4203. [CrossRef]
46. Cannizzaro, J.P.; Carder, K.L. Estimating chlorophyll a concentrations from remote sensing reflectance in optically shallow waters. *Remote Sens. Environ.* **2006**, *101*, 13–24. [CrossRef]

47. Schofield, O.; Grzymski, J.; Bissett, P.W.; Kirkpatrick, G.J.; Millie, D.F.; Moline, M.; Roeseler, C.S. Optical monitoring and forecasting systems for harmful algal blooms: Possibility or pipedream. *J. Phycol.* **1999**, *35*, 1477–1496. [CrossRef]
48. Jiang, R.; Wang, P.; Xu, Y.; Zhou, Z.; Luo, X.; Lan, Y.; Zhao, G.; Sanchez-Azofeifa, A.; Laakso, K. Assessing the operation parameters of a low-altitude UAV for the collection of NDVI values over a Paddy Rice Field. *Remote Sens.* **2020**, *12*, 1850. [CrossRef]
49. Lu, H.; Fan, T.; Ghimire, P.; Deng, L. Experimental evaluation and consistency comparison of UAV multispectral minisensors. *Remote Sens.* **2020**, *12*, 2542. [CrossRef]
50. Parrot. *SEQ-AN-02, Application Note: Pixel Value to Irradiance Using the Sensor Calibration Model*; Parrot: Paris, France, 2017; Volume SEQ-AN-01.
51. Lowe, G.D. Distinctive image features from scale-invariant keypoints. *Int. J. Comput. Vis.* **2004**, *20*, 91–110. [CrossRef]
52. Axler, R.; Will, N.; Ruzycki, E.; Henneck, J.; Olker, J.; Swintek, J. *Minnesota Lake Water Quality On-Line Database and Visualization Tools for Exploratory Trend Analyses*; Technical Report NRRI/TR-2009/28; University of Minnesota Duluth: Duluth, MN, USA, 2009.
53. American Public Health Association (APHA). *Standard Methods for the Examination of Water and Wastewater*, 21st ed.; American Public Health Association: Washington, DC, USA, 2005.
54. Song, B.G.; Park, K.G. Detection of aquatic plants using multispectral UAV imagery and vegetation index. *Remote Sens.* **2020**, *12*, 387. [CrossRef]
55. Xu, F.; Gao, Z.; Jiang, X.; Shang, W.; Ning, J.; Song, D.; Ai, J. A UAV and S2A data-based estimation of the initial biomass of green algae in the South Yellow Sea. *Mar. Pollut. Bull.* **2018**, *128*, 408–414. [CrossRef]
56. Jang, S.W.; Yoon, H.J.; Kwak, S.N.; Sohn, B.Y.; Kim, S.G.; Kim, D.H. Algal bloom monitoring using UAVs imagery. *Adv. Sci. Technol. Lett.* **2016**, *138*, 30–33.
57. Kim, H.M.; Yoon, H.J.; Jang, S.W.; Kwak, S.N.; Sohn, B.Y.; Kim, S.G.; Kim, D.H. Application of unmanned aerial vehicle imagery for algal bloom monitoring in river basin. *Int. J. Control Autom.* **2016**, *9*, 203–220. [CrossRef]
58. Gitelson, A.; Merzlyak, M.N. Quantitative estimation of chlorophyll-a using reflectance spectra: Experiments with autumn chestnut and maple leaves. *J. Photochem. Photobiol. B Biol.* **1994**, *22*, 247–252. [CrossRef]